Supporting Information for

2D Iron Oxide at the Graphene/SiC(0001) Interface

Ryotaro Sakakibara,[1] Tomo-o Terasawa,[2,3] Taizo Kawauchi,[4] Katsuyuki Fukutani,[2,3] Takahiro Ito,[5,6] and Wataru Norimatsu[7]*

[1] Research Center for Materials Nanoarchitectonics (MANA), National Institute for Materials Science (NIMS), Tsukuba 305-0044, Japan

[2] Advanced Science Research Center, Japan Atomic Energy Agency, Tokai 319-1195, Japan

[3] Institute of Industrial Science, The University of Tokyo, Tokyo 153-8505, Japan

[4] Isotope Science Center, The University of Tokyo, Tokyo 113-0032, Japan

[5] Department of Materials Science and Engineering, Nagoya University, Nagoya 464-8603, Japan

[6] Nagoya University Synchrotron Radiation Research Center (NUSR), Nagoya University, Nagoya 464-8603, Japan

[7] Faculty of Science and Engineering, Waseda University, Tokyo 169-8555, Japan

Correspondence should be addressed to R.S. (SAKAKIBARA.Ryotaro@nims.go.jp)

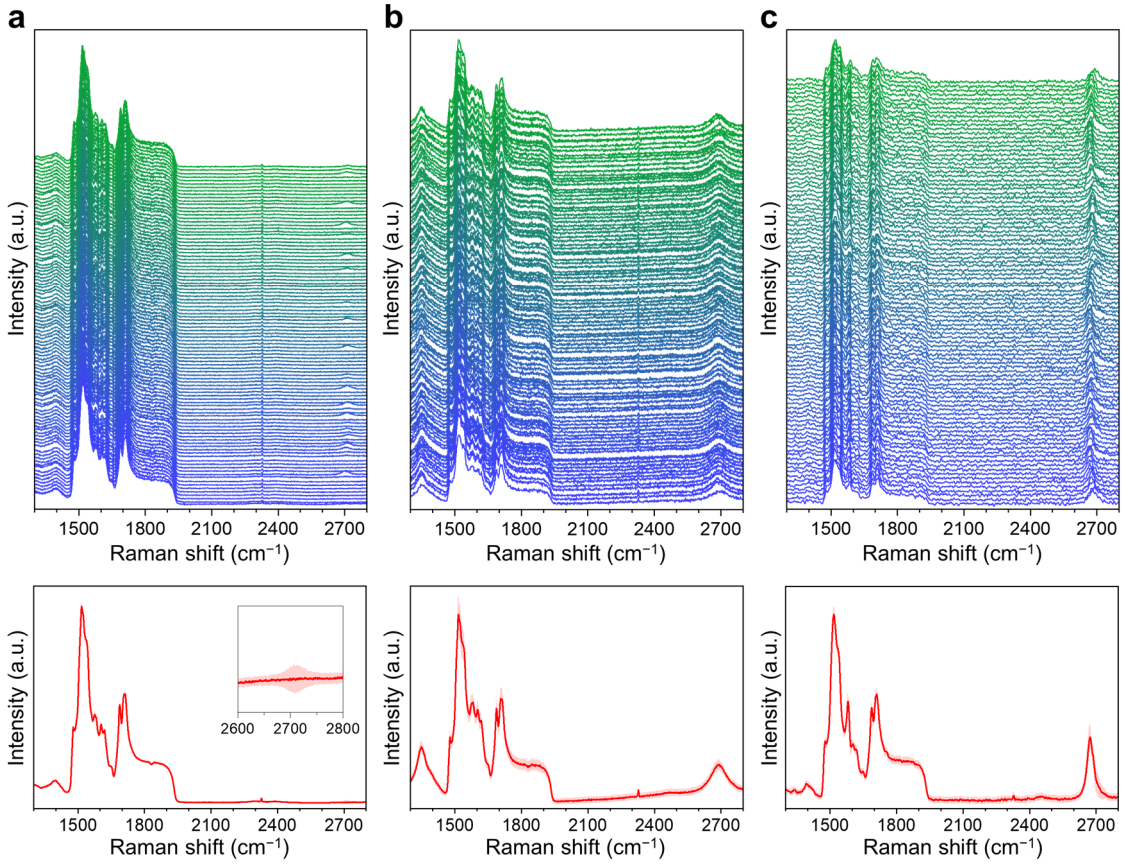

Figure S1. 100 individual Raman spectra (top) and the corresponding median spectra (bottom) for (a) the initial buffer layer sample, (b) the sample annealed with metallic Fe, and (c) the sample annealed with pre-oxidized Fe, shown without SiC subtraction. The pink shaded regions in the median spectra indicate ±1 standard deviation. The inset of the median spectrum of (a) shows a largely flat 2*D*-band region, indicating that the initial sample is mainly covered by the buffer layer with minor contributions from overgrown monolayer graphene.

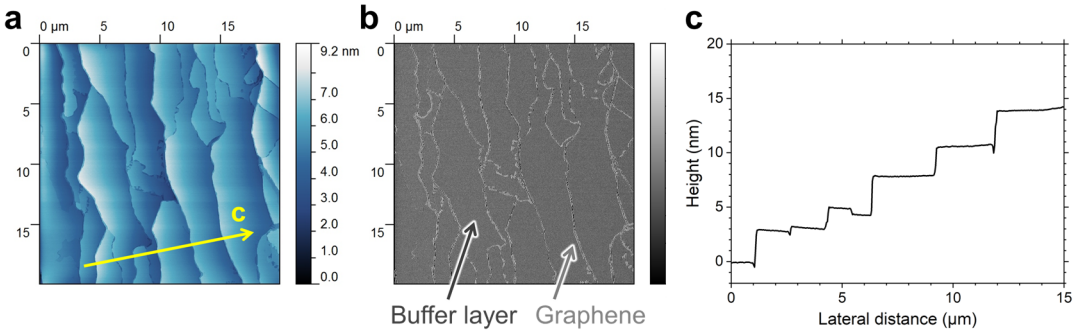

Figure S2. (a) Typical AFM topography image and (b) corresponding phase image of the initial buffer layer. (c) Height profile extracted along the yellow line in (a). In (b), dark and bright regions correspond to the buffer layer and partially grown monolayer graphene, respectively.

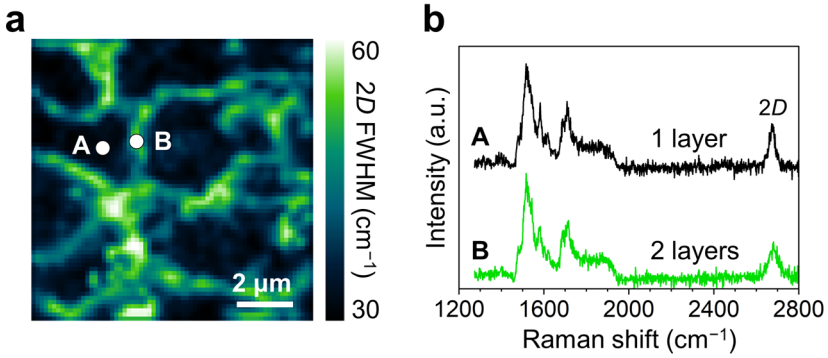

Figure S3. (a) Raman mapping image of the FWHM of the 2*D* band obtained from the sample annealed with pre-oxidized Fe. (b) Raman spectra extracted from the regions A and B in (a). The FWHM values in regions A and B are ~33 and ~55 cm^{-1}, which correspond to that of monolayer and bilayer graphene, respectively.[1–3]

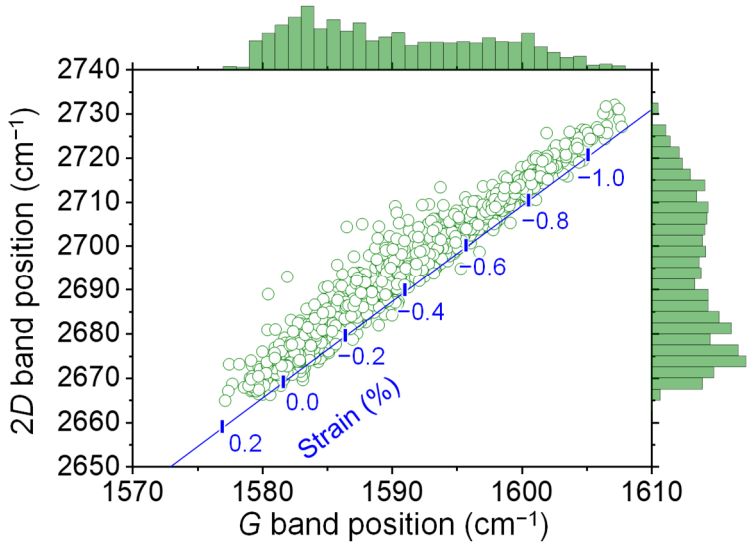

Figure S4. Statistical analysis[4] of the Raman mapping data shown in Figure S3. A linear correlation between the *G*-band and 2*D*-band positions is observed. The pronounced variation indicates that the graphene layer in this sample is subject to a wide range of compressive strain (0–1%). The 2*D* and *G* bands are shifted to higher and lower wavenumbers respectively, which cannot be explained solely by doping or strain effects. Similar anomalous shifts have been reported for the Ga intercalation system.[5] This behavior may indicate modifications of the phonon dispersion and/or Fermi velocity due to dielectric screening.[6]

	Peak	Position (eV)	FWHM (eV)
Figure 3a	SiC	283.67	1.06
	S1	284.50	1.10
	S2	285.38	1.30
	O	284.77	0.90
	C_xH_y	286.99	1.00
Figure 3e	SiC	283.22	1.07
	Gra	284.64	0.83
	C_xH_y	286.50	1.00
Figure 3i	SiC	282.84	0.75
	Gra	284.52	0.98
	X	–	–
	C_xH_y	286.94	0.90

Table S1. Fitting parameters for the XPS C 1*s* spectra. Since it is known that the S1 and S2 components of the buffer layer are separated by about 880 meV and exhibit a peak area ratio of 1 : 2, the peak fitting was performed under these constraints.[7–8] Component O represents the contribution from the overgrown monolayer graphene. Component X in the fitting of Figure 3i was obtained by scaling down the line shape of Figure 3a.

	Peak	Position (eV)	FWHM (eV)
Figure 3b	SiC	101.26	1.07
	Interface	101.66	1.07
Figure 3f	SiC	101.00	1.07
	Interface	102.37	1.10
	Fe–Si	99.84	0.85
Figure 3j	SiC	100.60	0.90
	Interface	101.77	1.05
	X	–	–

Table S2. Fitting parameters for the XPS Si 2*p* spectra. A spin-orbit splitting of 0.6 eV and an area ratio of $2p_{1/2}$ to $2p_{3/2}$ of 1 : 2 were applied in the fitting. Component X in the fitting of Figure 3j was obtained by scaling down the line shape of Figure 3b.

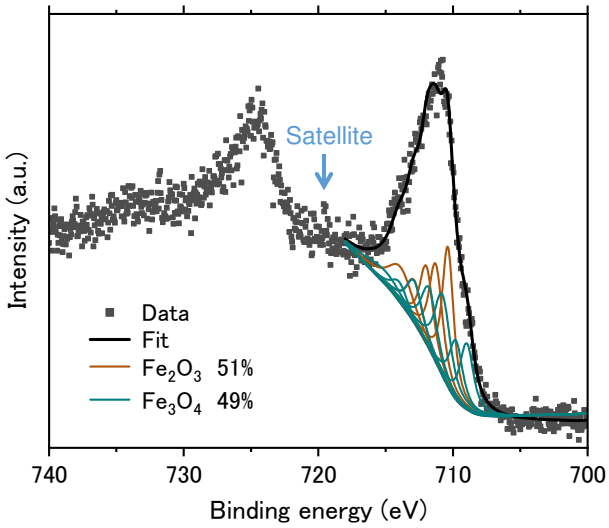

Figure S5. Tentative deconvolution of the Fe $2p_{3/2}$ spectrum shown in Figure 3k of the main text. The surface residue was assumed to be α-Fe_2O_3, whereas the interfacial component was tentatively assigned to Fe_3O_4 based on the Fe:O atomic ratio estimated from the calculated structures in Figure 7b,c of the main text. The fitting was carried out using an envelope-fitting approach with Biesinger's Fe $2p$ multiplet components.[9–10] In the fitting proceduce, the shake-up satellite peak indicated by the arrow was excluded because it overlaps with the Fe^{2+} component in the Fe $2p_{1/2}$ region.[10] After Shirley's background subtraction, five components for Fe_2O_3 (brown) and seven components for Fe_3O_4 (green) were included. The fitting was performed by fixing the relative peak positions, FWHM values, and area ratios within each phase. The fitting result suggests that a non-negligible amount of Fe_2O_3 residue remains on the surface.

	Peak	Position (eV)	FWHM (eV)
Figure S5	Fe_2O_3 #1	710.38	1.00
	Fe_2O_3 #2	711.28	1.20
	Fe_2O_3 #3	711.98	1.20
	Fe_2O_3 #4	712.88	1.40
	Fe_2O_3 #5	713.88	2.20
	Fe_3O_4 #1	708.98	1.20
	Fe_3O_4 #2	709.78	1.20
	Fe_3O_4 #3	710.78	1.40
	Fe_3O_4 #4	711.78	1.40
	Fe_3O_4 #5	712.88	1.40
	Fe_3O_4 #6	713.98	1.40
	Fe_3O_4 #7	715.08	3.30

Table S3. Fitting parameters for the Fe $2p_{3/2}$ spectrum of Figure S5, which are based on the multiplet components reported by Biesinger et al. [10]

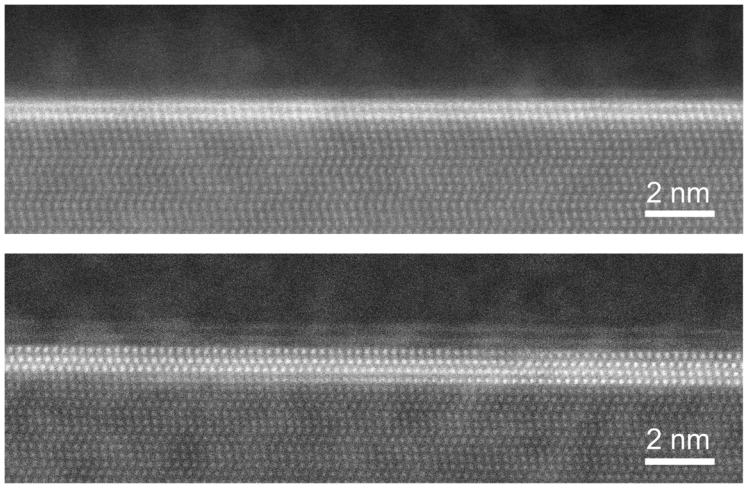

Figure S6. Cross-sectional HAADF-STEM images of the sample annealed with pre-oxidized Fe. The number of the interface layers varies from two to four in the observed area.

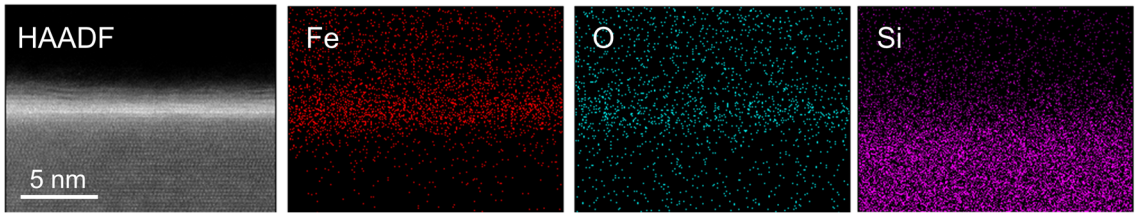

Figure S7. HAADF-STEM image and corresponding EDS elemental maps of Fe, O, and Si for the sample annealed with pre-oxidized Fe.

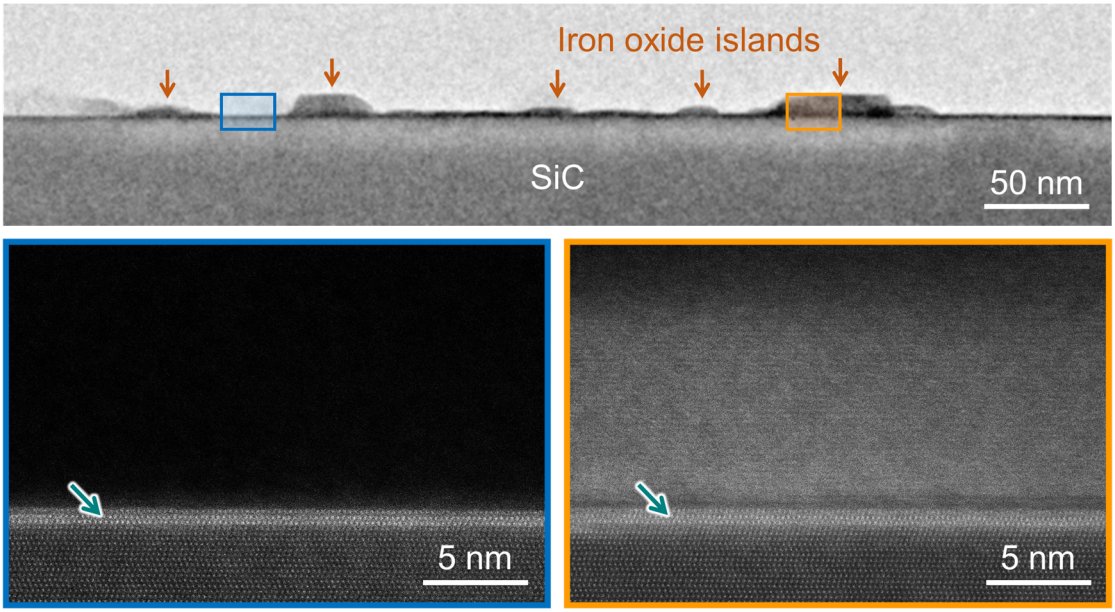

Figure S8. Low-magnification TEM image of the graphene/2D iron oxide/SiC sample, showing residual iron oxide islands distributed on the surface (brown arrows). High-magnification HAADF-STEM images reveal that the graphene/2D iron oxide/SiC structure is preserved regardless of the presence or absence of these residues, as indicated by the green arrows.

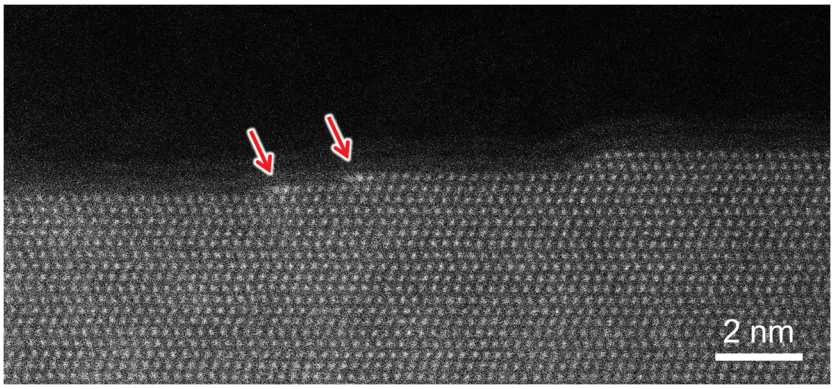

Figure S9. HAADF-STEM image of the intercalated sample, showing that bright spots of Fe atoms are observed only at the step edges, as indicated by the arrows.

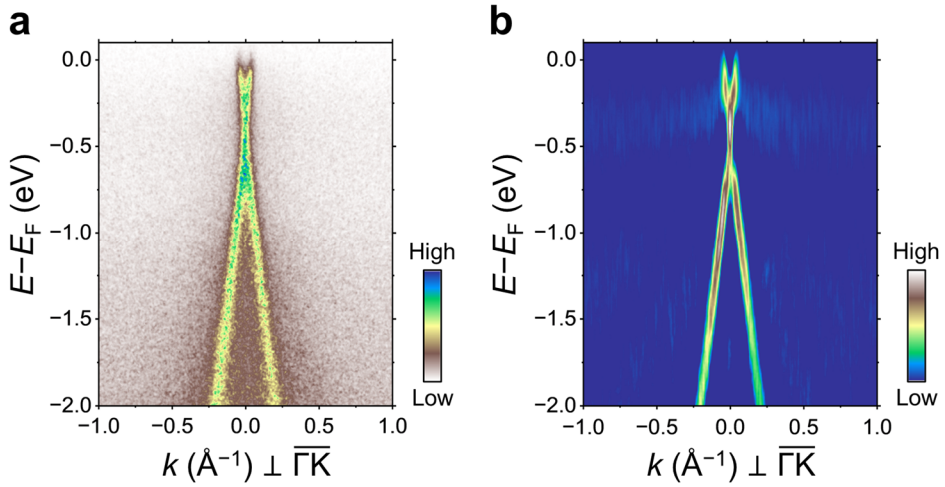

Figure S10. (a) ARPES *E–k* dispersion relation of epitaxial graphene on SiC acquired at a photon energy of 70 eV. (b) The corresponding second-derivative image. The Dirac point is located at about −0.4 eV relative to the Fermi energy, indicating electron doping induced by the underlying buffer layer.[11–12]

References

[1] A. C. Ferrari, Raman spectroscopy of graphene and graphite: Disorder, electron–phonon coupling, doping and nonadiabatic effects, *Solid State Commun.* **2007**, 143, 47.

[2] A. C. Ferrari, D. M. Basko, Raman spectroscopy as a versatile tool for studying the properties of graphene, *Nat. Nanotechnol.* **2013**, 8, 235.

[3] R. Sakakibara, W. Norimatsu, Microscopic mechanism of hydrogen intercalation: On the conversion of the buffer layer on SiC to graphene, *Phys. Rev. B* **2022**, 105, 235442.

[4] J. E. Lee, G. Ahn, J. Shim, Y. S. Lee, S. Ryu, Optical separation of mechanical strain from charge doping in graphene, *Nat. Commun.* **2012**, 3, 1024.

[5] S. Wundrack, D. Momeni, W. Dempwolf, N. Schmidt, K. Pierz, L. Michaliszyn, H. Spende, A. Schmidt, H. W. Schumacher, R. Stosch, A. Bakin, Liquid metal intercalation of epitaxial graphene: Large-area gallenene layer fabrication through gallium self-propagation at ambient conditions, *Phys. Rev. Mater.* **2021**, 5, 024006.

[6] F. Forster, A. Molina-Sanchez, S. Engels, A. Epping, K. Watanabe, T. Taniguchi, L. Wirtz, C. Stampfer, Dielectric screening of the Kohn anomaly of graphene on hexagonal boron nitride, *Phys. Rev. B* **2013**, 88, 085419.

[7] M. Ostler, R. J. Koch, F. Speck, F. Fromm, H. Vita, M. Hundhausen, K. Horn, T. Seyller, Decoupling the graphene buffer layer from SiC (0001) via interface oxidation, *Mater. Sci. Forum* **2012**, 717, 649.

[8] K. V. Emtsev, F. Speck, T. Seyller, L. Ley, J. D. Riley, Interaction, growth, and ordering of epitaxial graphene on SiC{0001} surfaces: A comparative photoelectron spectroscopy study, *Phys. Rev. B* **2008**, 77, 155303.

[9] A. Hughes, C. Easton, T. Gengenbach, M. Biesinger, M. Laleh, Interpretation of complex x-ray photoelectron peak shapes. I. Case study of Fe $2p_{3/2}$ spectra, *J. Vac. Sci. Technol. A* **2024**, 42, 053205.

[10] M. C. Biesinger, B. P. Payne, A. P. Grosvenor, L. W. M. Lau, A. R. Gerson, R. S. C. Smart, Resolving surface chemical states in XPS analysis of first row transition metals, oxides and hydroxides: Cr, Mn, Fe, Co and Ni, *Appl. Surf. Sci.* **2011**, 257, 2717.

[11] M. Kusunoki, W. Norimatsu, J. Bao, K. Morita, U. Starke, Growth and Features of Epitaxial Graphene on SiC, *J. Phys. Soc. Jpn.* **2015**, 84, 121014.

[12] J. Ristein, S. Mammadov, T. Seyller, Origin of doping in quasi-free-standing graphene on silicon carbide, *Phys. Rev. Lett.* **2012**, 108, 246104.